공학석사 학위논문

Hydrolysis of alginate into its monomers over sulfonated carbon catalyst derived from glucose

술폰산이 작용기화된 글루코오즈 유래 카본 촉매를 이용한 알지네이트 분해반응

2014 년 12 월

서울대학교 대학원

화학생물공학부

반 충 현

Abstract

Hydrolysis of alginate into its monomers over sulfonated carbon catalyst derived from glucose

Chunghyeon Ban

Master's program

School of Chemical and Biological Engineering

Seoul National University

To mitigate the global pollution and reliance on petroleum-based fuels and chemicals, various types of biomass, such as agricultural crops, wood, and algae, have been investigated. Among these biomass feedstocks, algae is considered as a

promising renewable resource due to its rapid growth, inedibility, and ligin-free composition.

Alginate, the major constituent of algae, has found its wide applications in numerous fields. Similar to the structure of cellulose composed of glucoses via 1,4-glycosidic linkage, alginate consists of two hexuronic acids, β–D–mannuronic acid and α–L–guluronic acid by the ether bond. With the structural analogy, alginate can also be subjected to the current biorefinery technology, namely, hydrothermal conversion, to produce value-added organic compounds. To hydrolyze biomass effectively, employing of acid catalysts is essential. The use of homogeneous catalysts, however, causes critical issues, such as separation, purification, and neutralization. In this sense, developing solid acid catalysts easily separable and having a high catalytic activity has drawn interest worldwide.

In this work, hydrothermal depolymerization of alginates into its two monomers over sugar-derived solid acid catalysts was performed to investigate effects of catalyst properties, such as acid density, specific surface area, and thermal stability, on the yield of monomers. The catalysts bearing three functional groups, phenolic OH, -COOH and -SO_3H, were synthesized by partial carbonization of D-glucose and sulfonation. It was found that the presence of strong brønsted acid sites(-SO_3H) catalyzed hydrolysis of alginate, whereas weak acid sites(-OH and -COOH) had negligible effect on the reaction. The heterogeneous carbon catalyst shows a comparable activity with that of homogeneous catalysts such as sulfuric acid. The high activity is explained by high acid density and hydrophilic surface of the

catalyst, despite low surface area. The sulfonated carbon shows the possibility of replacing homogeneous catalysts and could propose a green route to decompose alginate.

Keywords: Alginate hydrolysis, Mannuronic acid, Guluronic acid, Sulfonated carbon catalyst

Student Number: 2013-20973

Contents

List of Tables

List of Figures

Chapter 1. Introduction

1.1. Background

An imprudent consumption of petroleum–based fuels and chemicals has been escalating the depletion of limited crude oil reservoir. In addition, it has resulted in critical environmental issues such as pollution, emission of greenhouse gases and thus global warming[1]. In order to reduce the world's heavy reliance on the traditional petrochemicals and to mitigate the climate change, investment in developing alternative energy has increased since 2000[2]. The portion of sustainable energy in global power generation is projected to grow substantially in the near future[3, 4]. In recent years, solar, wind, tidal, hydro, geothermal, biomass and other sources have been utilized as renewable energy[5, 6]. Among the aforementioned renewables, biomass is indubitably the only source to direct produce carbon–based materials[7].

The first–generation biofuels and chemicals rely on edible crops. These starch–based feedstocks, however, have competed with the food supply and forced the next generations of biomass to be developed. Non–edible feedstocks, i.e. lignocellulosic biomass, are often referred to as the second–generation biomass. These materials are comprised of polysaccharides and lignin. Unfortunately, lignin intertwined with polysaccharides gives it recalcitrant properties to decomposition

and makes it more difficult to produce biofuels and chemicals than the first– and third–generation biomass[8]. The algal biomass known to be the third generation biomass is considered as a promising alternative resource since it grows faster and needs less amount of arable land area than their terrestrial cousins[9]. Furthermore, the absence of lignin in algae makes it straightforward to degrade it. Several approaches have been made to decompose various types of biomass. Enzymatic hydrolysis[10], pyrolysis[11-13], and acid-catalyzed hydrolysis in water[14, 15] and ionic liquids[16, 17] are common techniques applied to yield valuable compounds such as bio-oil, ethanol, or reducing sugars from lignocellulosic biomass.

In 2004, U.S. Department of Energy (DOE) reported top 12 value-added chemicals derived from sugars[18]. The chemicals selected include lactic acid, succinic acid, levulinic acid, malic acid and so forth. These biomass-derived chemicals can further be transformed into high-value chemicals. Some of the selected organic acids could be produced from the third generation biomass, algae. A few research groups depolymerized alginates under sub– and supercritical conditions[19-21] in an effort to displace cellulose for the production of the aforestated organic acids, e.g. succinic acid, lactic acid, malic acid, and formic acid recently[21].

1.2. Structure of Alginate

Alginate, unbranched bio-copolymers isolated from brown algae, has found their applications in numerous fields. For instance, it has been used as a thickener, stabilizer, gelling agent, and emulsifying agent in food industry. It has also been utilized in pharmaceutical industry as a drug deliver, dressing, and dental fillings[22]. Similar to the structure of cellulose comprised of glucoses by 1,4–glycosidic bond, alginate, as shown in Figure 1, consists of two uronic acids, β–D–mannuronic acid (M) and α–L–guluronic acid (G) via the ether bond[22-26]. The amount of respective monomers and sequential distribution vary depending on its source, and the arrangement of two urnoic acids in alginates was elucidated by ^{1}H NMR[27-29] and FT-IR[30] elsewhere. Three different types of blocks in alginates are as follows: two homopolymeric blocks and alternating blocks (MM, GG or MG). Because of two–fold helical structure, G blocks are more rigid than the others[22, 31, 32].

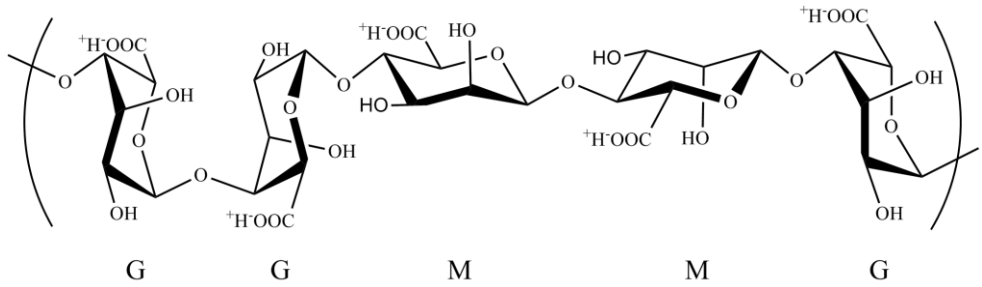

Figure 1. Structure of alginate

1.3. Objective

With the structural analogy to cellulose, alginate can also be applied to the existing biorefinery technologies, viz. hydrothermal conversion, to produce valuable chemicals. As glucose, a monomer of cellulose, is regarded as an alternative building block for the production of chemicals and fuels, alginate's monomers are expected to be versatile intermediate chemicals to higher value products. Thus, it is of great importance to selectively hydrolyze alginate into its monomers for the better utilization of the third generation biomass.

For the effective hydrolysis of alginate, employing of acid catalysts is essential. Several attempts, for instance, have been made to convert alginate into its monomers or uronic acid blocks by employing sulfuric acid[33, 34] and oxalic acid[35]. The use of these homogeneous acid catalysts, however, poses significant challenges of product separation, waste purification, and corrosion of reactors. In this respect, developing solid acid catalysts with an easy separability and a high catalytic activity has attracted interest worldwide.

To date, various sugar-derived carbon materials were studied[36-47] and found to be well qualified to hydrolyze biomass feedstocks owing to their hydrothermal stability. In addition, they are insoluble in most of solvents, e.g. water, methanol, and dimethylformamide which makes separation processes simple[48]. Furthermore, in terms of glucose yield, acid-functionalized carbon materials showed comparable catalytic activities with those of homogeneous acid catalyst,

sulfuric acid.

To my knowledge, hydrolysis of alginate over solid acid catalysts has never been reported. The scope of this research is, hence, to hydrothermally decompose alginate into its two monomers, versatile intermediate chemicals, over acid-functionalized carbon catalysts derived from glucose. In addition, catalytic activities of synthesized solid catalysts were compared with those of homogeneous acid catalysts, sulfuric acid, and other commercial solid acid catalysts

Chapter 2. Experimental

2.1. Preparation of catalysts

Glucose-derived carbon catalysts bearing functional groups of –OH, –COOH, and $–SO_3H$ were prepared referring to previously reported methods with modification[41, 43, 45, 46, 49-52].

2.1.1. Partial carbonization of glucose (Glu)

10g of D-glucose was charged into a 300 ml of glass reactor with a 3-neck lid. Before partial carbonization, the reactor was purged with N_2 flow (40ccm) for 1hr. The reactor was, then, heated at 400℃ for 16hr under N_2 flow (40ccm). The resulting brown-black solid was ground to powder, filtered and washed with more than 3L of hot distilled water (≥80℃) followed by oven-drying at 100℃ overnight. The resulting carbon is referred to as Glu hereinafter.

2.1.2. Sulfonation of carbons derived from glucose (Glu-SO_3H)

1.5g of glucose-derived carbons was added to 30ml of concentrated sulfuric acid (95%, 17.8M) in a glass flask (100ml). Before the sulfonation, the flask was purged with N_2 flow (40ccm) for 1hr. The mixture was heated at 150℃ under N_2 flow (40ccm). After 16hr, the sulfonated carbons were filtrated and washed with 3

L of hot distilled water until the washing became neutral (≥80℃). The resultant acid-functionalized carbon catalyst is named Glu-SO_3H hereafter.

2.2. Characterization of the acid-functionalized carbon catalysts

2.2.1. ^{13}C cross-polarization/magic angle spinning nuclear magnetic resonance (CP/MAS NMR)

^{13}C CP/MAS NMR spectra were recorded by Bruker AVANCE 400 WB (400 MHz) with a 4-mm probehead with a spectrometer frequency and spinning rate of 100.6 MHz and 7 kHz, respectively.

2.2.2. Diffuse reflectance infrared fourier transform spectroscopy (DRIFTs)

FT-IR spectra were recorded using Nicolet iS50 FT-IR spectrometer between 600 and 4000 cm^{-1} with resolution of 4cm^{-1}.

2.2.3. X-ray diffraction (XRD)

X-ray diffraction patterns of catalysts were obtained by Rigaku diffractometer employing Cu K α radiation with X-ray generating voltage and current of 40kV, 30mA, respectively. The patterns were recorded from 5 to 60° with a scanning step

size of 0.02.

2.2.4. Elemental analysis

To determined chemical composition of the catalysts and sulfur content on the catalyst after sulfonation, elemental analysis was performed on Elemental Analyzer (Thermo Fischer) with a CHNS–Porapack PQS column.

2.2.5. Back titration

The Brønsted acid density of catalysts in an aqueous medium was measured by back titration method. Back titration method was described elsewhere[52, 53]. Typically, a catalyst (0.05 g) was added into 15 ml of NaOH solution (0.01M). The solution was agitated for 1hr at room temperature and subjected to a centrifugal action. The supernatant was titrated by HCl solution (0.02M) with a drop of phenolphthalein solution (0.5 wt% in ethanol:water (1:1)).

2.2.6. N_2 adsorption–desorption

N_2 adsorption–desorption was applied to investigate the specific surface area of prepared catalysts using Micrometritics ASAP 2010 apparatus at –196℃. Glu and Glu-SO_3H were degassed under N_2 flow at 350℃ and 250℃, respectively, for more than 12 hours. The specific surface area of the catalysts were measured by Brunauer–Emmett–Teller (BET) method.

2.2.7. Inductively coupled plasma–atomic emission spectroscopy (ICP–AES)

ICP–AES was employed to measure the amount of sulfur leached from Glu-SO_3H after hydrolysis reactions. After a centrifugal action, the supernatants of product mixtures were diluted by 20 times to a total volume of 4mL and analyzed by PerkinElmer/Optima–4300 DV.

2.2.8. Thermogravimetric analysis (TGA)

Thermogravimetric curves were recorded using SDT Q600 (TA Instruments) under N_2 flow (100ccm) from room temperature to 800℃ with a ramping rate of 10℃/min.

2.2.9. Adsorption of alginate and glucuronic acid onto the prepared catalyst

Adsorption capacity of catalysts was tested referring to a method reported elsewhere[54] and the method was modified. Glucuronic acid was used as a surrogate monomer of alginate herein. 0.05g of Glu-SO_3H was added into each of 2 vials (20ml) containing 10 ml of 0.5% (w/v) sodium alginate solution and 0.5% (w/v) glucuronic acid solution, respectively. The mixtures were then agitated at room temperature by means of a magnetic stirrer at 400 rpm. At the time of 10, 20,

40, 80, 120 min, and 15hr, supernatants were taken from each vial, centrifuged and analyzed by HPLC to determine the concentration of non-adsorbed sodium alginate and glucuronic acid.

2.2.10. Gel permeation chromatography (GPC)

Gel permeation chromatography was conducted by Ultimate 3000 (Dionex) equipped with reflective index (RI) detector and a series of three columns, Waters Ultrahydrogel 120, 150, and 1000 maintained at 40℃. 0.1M of sodium azide solution was used as a mobile phase at a flow rate of 1.0 ml/min. Pullulan having a molecular weight distribution from 342 to 80,500 was used to calibrate GPC.

2.2.11. High performance liquid chromatography (HPLC)

The concentrations of mannuronic acid, guluronic acid, and other water soluble organic compounds in aqueous phase after reactions were measured by a high performance liquid chromatography (HPLC) system equipped with Agilent quaternary pump, ultraviolet-visible (UV/VIS) detector, RI detector, degasser, and two columns of Shodex KC-811 maintained at 40℃. 5mM of H_3PO_4 was used as a mobile phase at a flow rate of 1.0 ml/min. Temperature of the RI detector was set at 55℃. Every liquid product was diluted by 20 before injected to HPLC system.

Carbon-based yields of alginate's monomers and other water soluble organic

compounds were calculated referring to the equation below[55].

Carbon yield of monomers (%) = 100 × (moles of monomers in the product / moles of monomer units in charged alginates)

Carbon yield of water soluble organic compounds (%) = 100 × (number of carbon atoms in an organic compound / 6) × (moles of an organic compound in the product / moles of monomer units in charged alginates)

2.2.12. Reactor and hydrolysis conditions

All hydrolysis reactions were conducted in SUS316 tubular reactors (Swagelok) with inner volume of 4mL. 1.2mL of 1% (w/v) of sodium alginate solution prepared beforehand was charged into the reactor with a magnetic stirrer. The reactor is then immersed into an oil bath maintained at different temperatures (100, 120, and 140℃) for desired reaction times with stirring rate of 400 rpm. After the reaction, the reactor was quenched to room temperature to prevent further degradation.

2.2.13. Durability experiments of the sulfonated carbon catalyst

Durability of the Glu-SO_3H catalyst was investigated over four repeated cycles. After each reaction, the catalyst was retrieved, filtered, and washed with distilled water and ethanol repeatedly. Then, the catalyst was oven dried at least 1hr.

The oven-dried used catalyst was then employed in the same manner mentioned above.

Chapter 3. Result and discussion

3.1. Characteristics of the prepared carbon catalysts

XRD patterns of Glu and Glu-SO_3H catalysts are shown in Figure 2. The XRD patterns show two weak broad peaks at 20–30° and 40–50°, which are assignable to graphitic (002) and (101) reflection, respectively. These diffraction peaks indicate that both catalysts are comprised of polyaromatic amorphous carbon sheets in a disordered fashion[56, 57], and there is no distinctive difference in XRD patterns before and after sulfonation of Glu catalyst. This implies that the carbon catalyst retains its structure after sulfonation. To further investigate the structure of the catalysts, ^{13}C CP/MAS NMR spectroscopy was employed.

^{13}C CP/MAS NMR spectra of the catalysts are displayed in Figure 3. Two broad peaks appeared at 127 ppm with sidebands (at 57 and 197 ppm) and 150 ppm, which are assignable to polycyclic aromatic carbon atoms[44, 51, 58], and phenolic OH group, respectively. No peak attributable to C–O–C was observed at 72 ppm [43]. These results suggest that the prepared catalysts are sp^2-derived polycyclic aromatic carbons with phenolic OH moiety. A peak at 180 ppm assignable to carboxylic groups were concealed by a weak broad peak of spinning sideband. In addition, a resonance peak for carbon atoms bearing SO_3H group (at 140 ppm)

could not be recognized in NMR spectrum of Glu-SO_3H because of the intense broad signal of aromatic carbon atoms at 127 ppm[40]. Hence, FT-IR spectroscopy was performed to confirm the presence of COOH and SO_3H groups in the catalysts.

As shown in Figure 4, adsorption peaks at 1181 and 1032 cm^{-1} attributed to SO_3^- and O=S=O stretching, respectively[49, 51], were observed for Glu-SO_3H catalyst. This suggests that sulfonate groups were introduced after sulfonation of carbonized glucose. Adsorption signals at 1600, 1700, and 2920 cm^{-1} for both catalysts are assigned to stretching bands of C=C[59], C=O[51], and C–H[60], respectively. These indicate the presence of aromatic carbons with carboxylic groups.

To sum up, incomplete carbonization of glucose followed by sulfonation yielded polycyclic aromatic carbons bearing functional groups of –OH, –COOH, and –SO_3H linked by sp-2 carbons.

Sulfur content and acid density of Glu-SO_3H catalyst were determined by elemental analysis and back titration (Table 1). It is widely known that all sulfur atoms presence in sulfonate groups on sulfonated carbons according to X-ray photoelectron spectroscopy[44]. The same would be applied to the case of Glu-SO_3H prepared in this work. Glu-SO_3H catalyst has sulfur content of 0.797 mmol/g and acid density of 2.93 mmol/g, whereas Glu has neutral property despite the presence of phenolic OH and carboxylic acid. BET surface area of Glu and Glu-SO_3H catalysts are relatively small (< 2 m^2/g).

Thermogravimetric curves show thermal stability of catalysts under N_2

atmosphere. As displayed in Figure 5, a slight weight loss was observed for both catalysts at approximately 100℃, which was due to desorption of water absorbed onto the catalysts[61]. However, Glu-SO_3H catalyst showed a significant weight loss above 200℃, which was caused by decomposition of sulfonate groups[61] and gasification of Glu-SO_3H catalyst[62].

A hypothesis that a reaction rate of cellulose hydrolysis with solid catalysts depends on adsorption capability of catalysts has been verified by adsorbing a reactant, cellobiose, onto a sulfonated resin catalyst[63]. In addition, it was proposed that hydrophilic binding sites on a catalyst favored a molecule having more hydrophilic groups. In other words, alginate would be preferably adsorbed onto the Glu-SO_3H surface compared with its monomers. Herein, the same was applied by adsorbing alginate and glucuronic acid as a surrogate monomer onto the Glu-SO_3H surface. In this case, hydrophilic –OH and –COOH groups serve as a binding site and SO_3H groups act as a catalytic site. As displayed in Figure 6, adsorption curves show that approximately 2% of alginate was adsorbed onto Glu-SO_3H and the curve reached a plateau, whereas none of glucuronic acid was adsorbed. From this result, it can be concluded that alginate could be easily attracted onto the Glu-SO_3H surface and alginate's monomers produced would be selectively desorbed after the hydrolysis giving unreacted alginates new free surface to adsorb, which increases a catalytic activity.

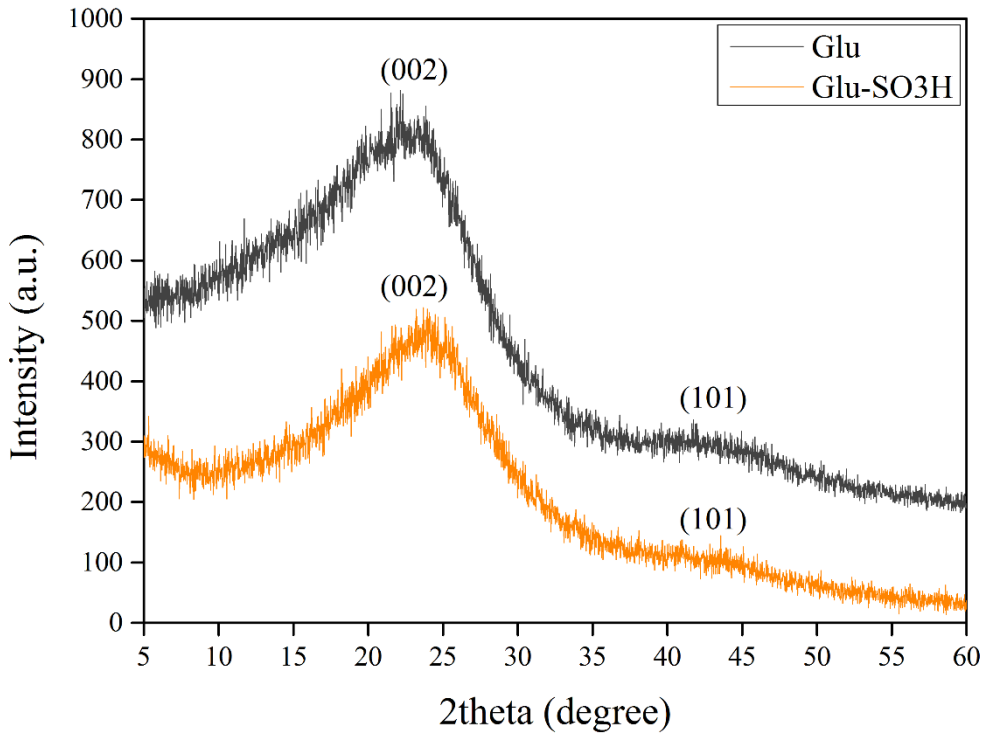

Figure 2. XRD patterns of the carbon catalysts.

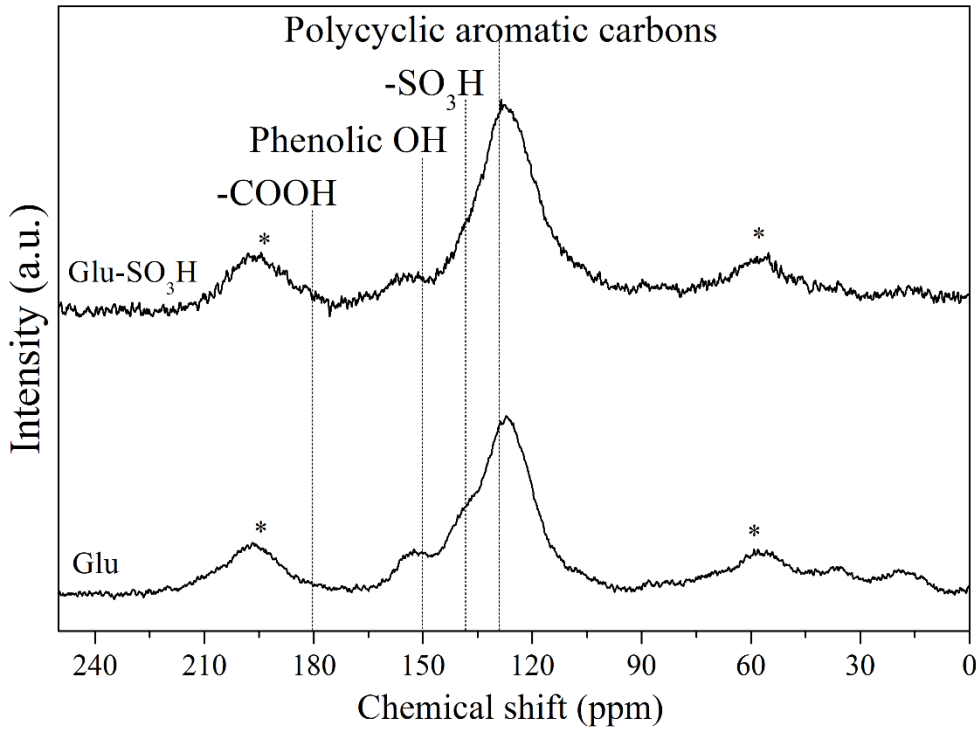

Figure 3. ^{13}C CP/MAS NMR spectra of the catalysts.

* spinning sidebands appear at 57 and 197 ppm

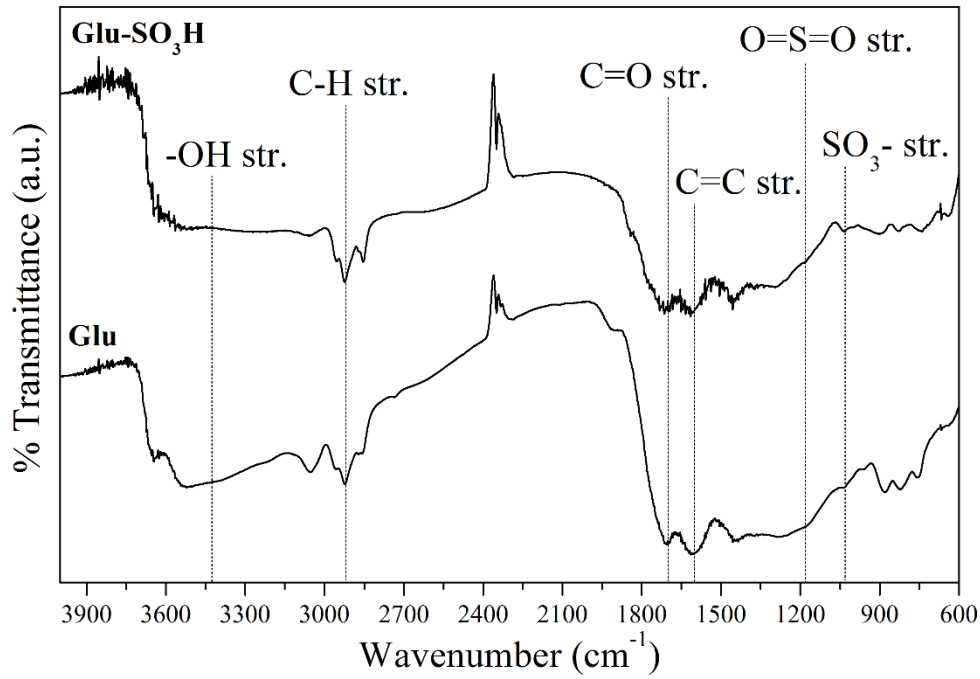

Figure 4. FT-IR Spectra of Glu and Glu-SO_3H catalysts.

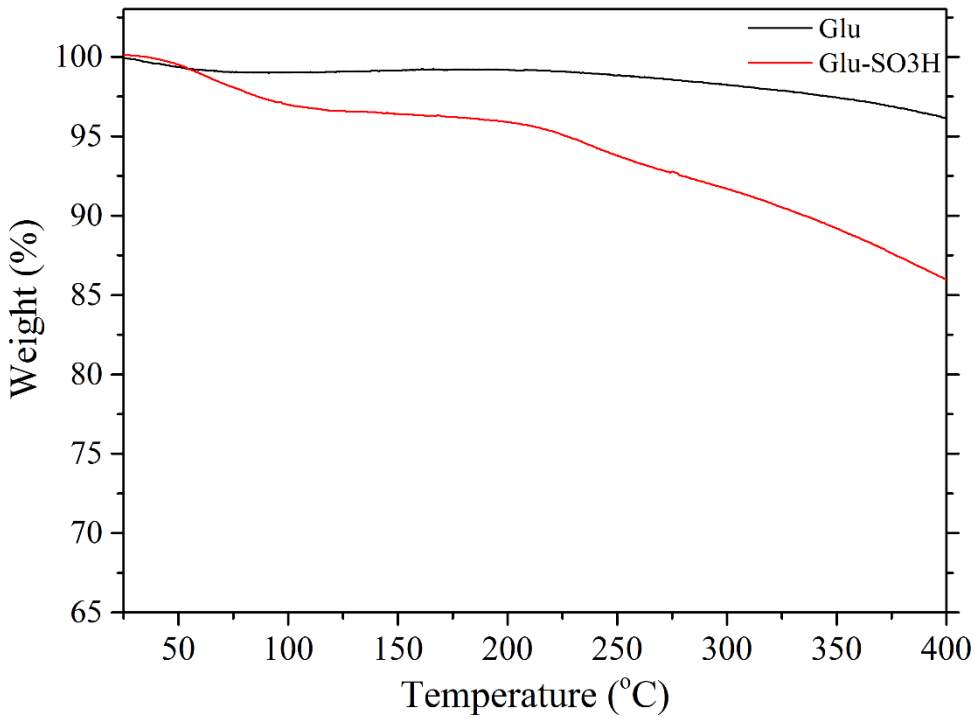

Figure 5. Thermogravimetric curves of the carbon catalysts.

Table 1 Chemical compositions, acid density, and surface area of catalysts before and after sulfonation

Catalyst	Chemical composition [a]	Sulfur amount [b] (mmol/g)	Acid density [c] (mmol/g)	Surface area [d] (m^2/g)
H_2SO_4	-	-	20.39	-
Glu	$CH_{0.5}O_{0.12}$	-	-	1.9
Glu-SO_3H	$CH_{0.45}O_{0.37}S_{0.01}$	0.767	2.93	0.5

[a] Chemical compositions were determined by elemental analysis.

[b] Sulfur amount was determined by elemental analysis.

[c] Acid amount was measured by back titration.

[d] Specific surface area was measured by Brunauer–Emmett–Teller method

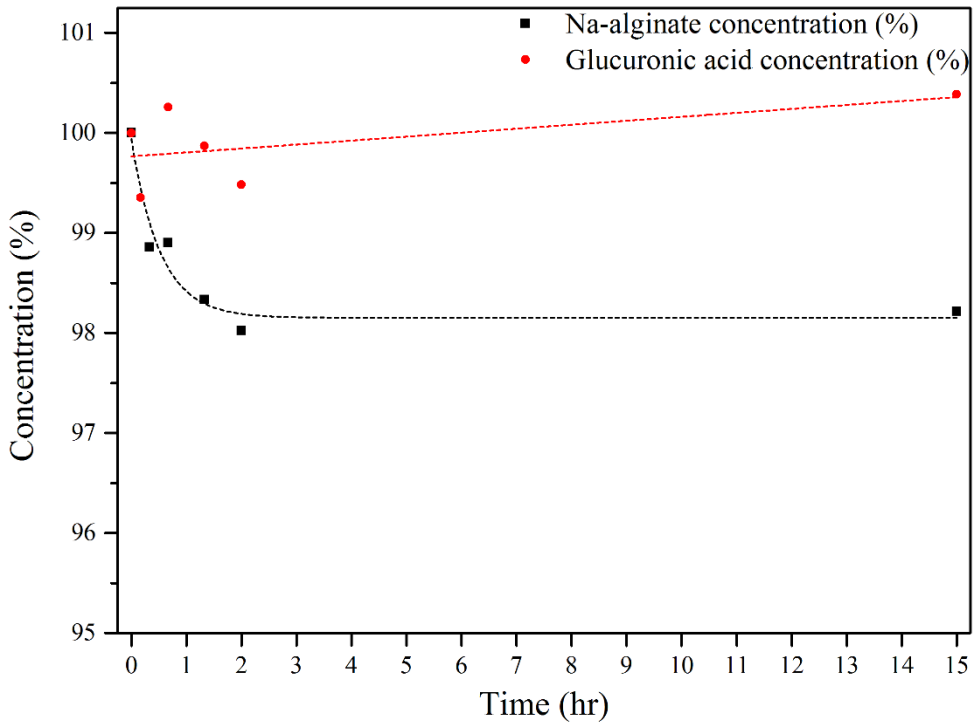

Figure 6. Adsorption curves of Na-alginate and glucuronic acid onto Glu-SO_3H catalyst.

3.2. Hydrolysis of alginate using sulfuric acid and the sulfonated carbon catalyst

It has been confirmed that hydrolysis of alginate occurs by cleavage of 1,4-glycosidic linkage which was verified by FT-IR spectroscopy[64]. The break of the ether bonds yields alginate's two monomers. The extent of depolymerization of alginate during the hydrolysis reaction was observed by GPC (Figure 7–10). As the reaction temperature and time increased, alginate having average molecular weight of 30kDa was degraded into smaller molecules even in the absence of homogeneous and heterogeneous acid catalysts. This is partly due to properties of subcritical water. At an elevated temperature, the concentration of proton ion increases owing to high value of ion product of water (K_W) and thus water could catalyze the reactions at higher temperatures (120 and 140℃)[65]. However, the activity of subcritical water was not comparable to that of H_2SO_4. As displayed in Figure 9, Glu catalyst has little effect on the depolymerization of alginate as the subcritical water did. Comparing Figure 8 with 10, depolymerization rates are similar for both reactions using H_2SO_4 and Glu-SO_3H. Referring to the GPC results, it is believed that the amounts of monomers reached their maxima within 16hr and 1hr when reactions were conducted at 120 and 140℃, respectively. To further investigate hydrolysis of alginate and production of other organic compounds, GC-MS analysis was conducted.

The similar trends of alginate depolymerization were obtained by GC-MS analysis. Total ion chromatograms (TIC) of GC-MS were displayed in Figure 11–

13. Monomers were eluted between the shaded region, 33 and 36 min. At high temperatures (120 and 140℃) for prolonged reaction times over Glu-SO_3H, further degradation of monomers arose and production of byproducts became prominent, whereas reactions at low temperature (100℃) produced solely monomers. A few organic acids were produced as unwanted byproducts such as oxalic acid, malic acid, succinic acid, tartaric acid, and pyruvic acid. Acetic acid and furfural couldn't be detected by GC-MS since acetic acid was highly volatile and furfural was not derivatized by the aforementioned method. Reaction conditions where these organic acids were yielded vary among the compounds. For instance, 5-keto-D-glutaric acid was produced only when the hydrolysis proceeded over 12hr at 120℃. To quantify alginate's monomers and few byproducts, HPLC was performed.

HPLC chromatograms of hydrolyzates were displayed in Figure 14 and 15. In the HPLC system used in this work, monomers, especially mannuronic acid, couldn't be clearly baseline separated since a peak at 12.008 min assignable to mannuronic acid was obscured by an unknown broad peak near 12 min. The unknown peak protruded obviously as the reaction temperature and time increased. The unknown, however, is presumed to be an isomer of mannuronic acid or guluronic acid. This presumption can be supported by GC-MS analysis. Judging from the similarity among mass spectra (Figure 17 and 18) of each compound eluted at different retention times, 9 major peaks in TIC of GC-MS could be classified into four distinct groups (Figure 16) and all groups were identified as different isomers of hexuronic acids, such as galacturonic acid and glucuronic acid. Thus, the unknown in HPLC chromatograms can be regarded as an isomer of

mannuronic acid or guluronic acid considering that the given HPLC system was not able to separate isomers. Assuming that the unknown peak near 12 min in Figure 14 and 15 was an isomer convertible into mannuronic acid and that tangents of calibration curves of hexuronic acids were identical, quantification of monomers proceeded with those two peaks. Carbon-based yields of monomers obtained by HPLC quantification are shown in Figure 19–21.

Glu-SO_3H, with regard to monomer production, exhibits the higher total monomer yield than sulfuric acid at high temperatures (120 and 140℃). As shown in Figure 20 and 21, this is explained by the fact that produced monomers were further decomposed to smaller compounds such as acetic acid and furfural when sulfuric acid was employed. The adsorption capability of the Glu-SO_3H catalyst accounts for the good catalytic activity despite the low surface area. As described in the adsorption experiment, hydrophilic surface of the catalyst selectively attracts alginate and easily diffuses produced monomers out. This prevents unwanted side reactions from occurring. In every reaction, the yield of mannuronic acid is always higher than that of guluronic acid. This is due to the two-fold helical structure of guluronic acid blocks making them recalcitrant to hydrolysis[22, 31, 32].

The highest total monomer yields were observed for the reactions for 16hr at 120℃ and for 1hr at 140℃ over Glu-SO_3H catalyst. Therefore, comparative experiments with commercial solid acid catalysts were performed at those reaction conditions, hereinafter.

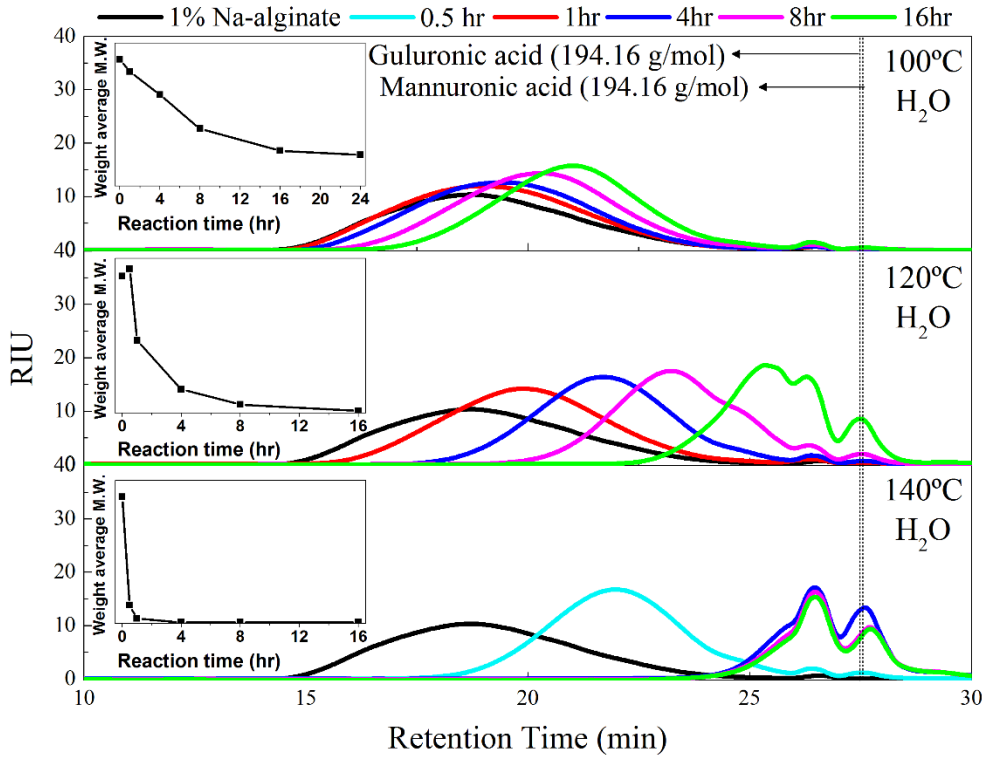

Figure 7. GPC chromatograms of hydrolyzates reacted at different reaction temperatures in H_2O.

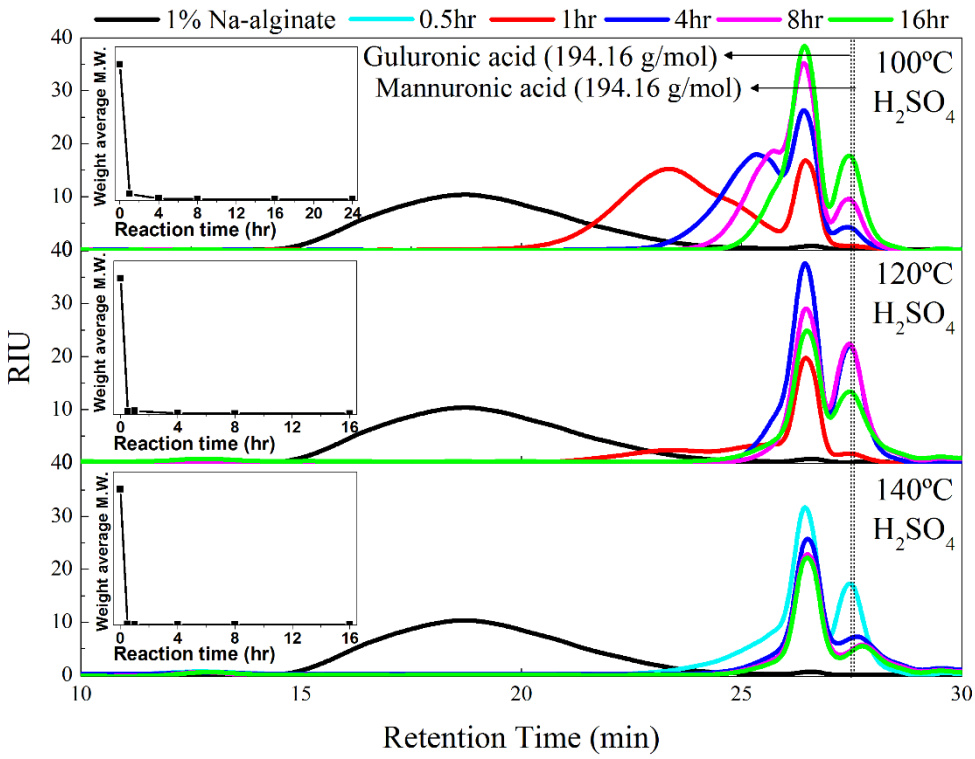

Figure 8. GPC chromatograms of hydrolyzates reacted at different reaction temperatures in H_2SO_4.

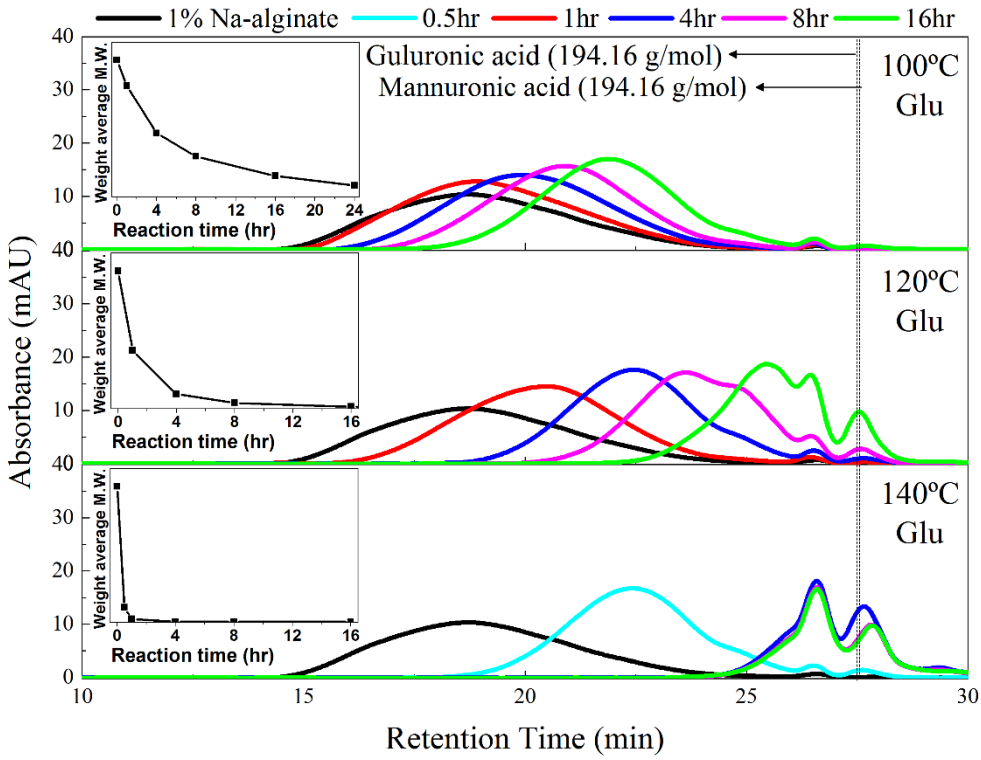

Figure 9. GPC chromatograms of hydrolyzates reacted at different reaction temperatures over the Glu catalyst.

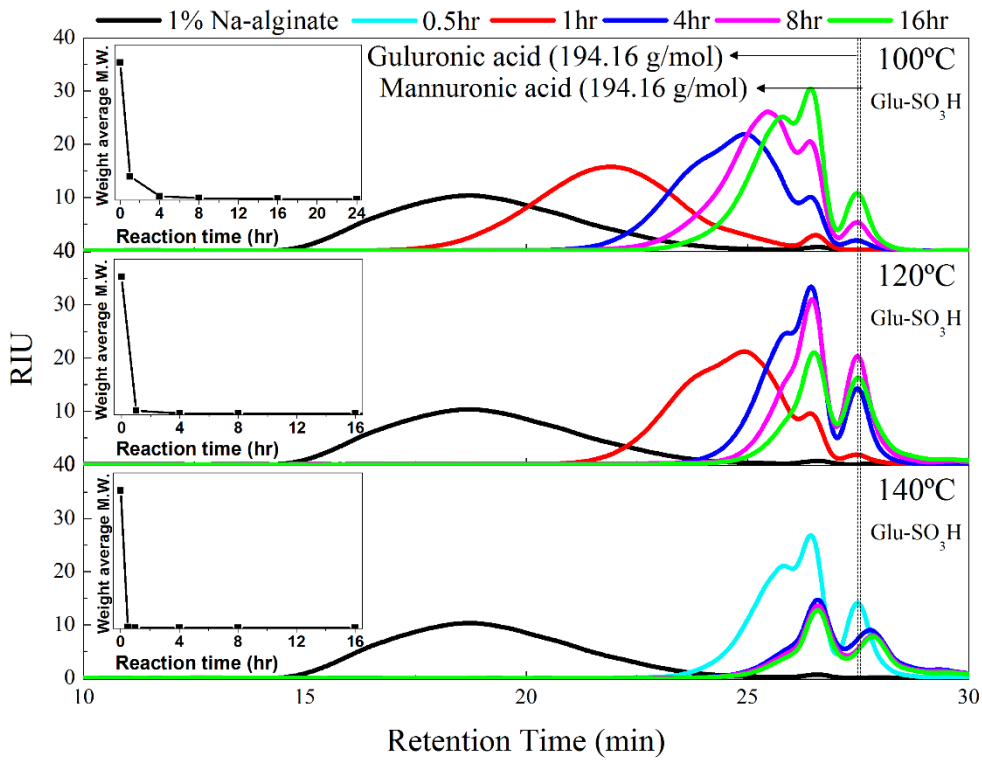

Figure 10. GPC chromatograms of hydrolyzates reacted at different reaction temperatures over the Glu-SO_3H catalyst.

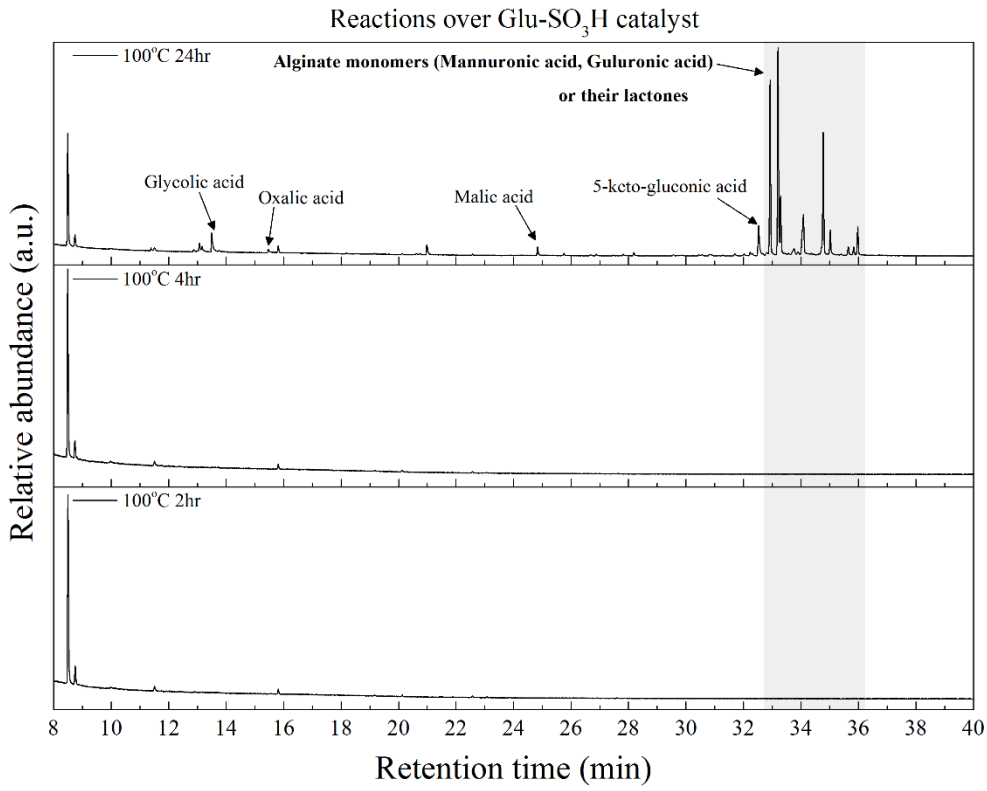

Figure 11. GC-MS total ion chromatograms of hydrolyzates reacted at 100℃ over Glu-SO_3H

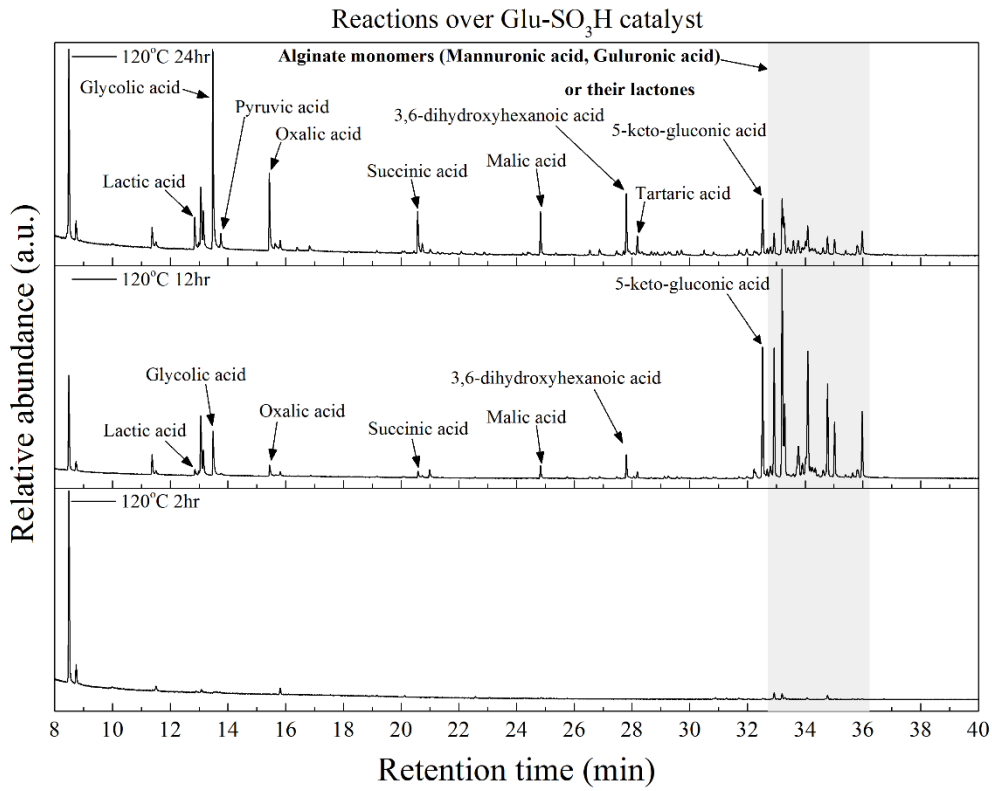

Figure 12. GC-MS total ion chromatograms of hydrolyzates reacted at 120℃ over Glu-SO_3H

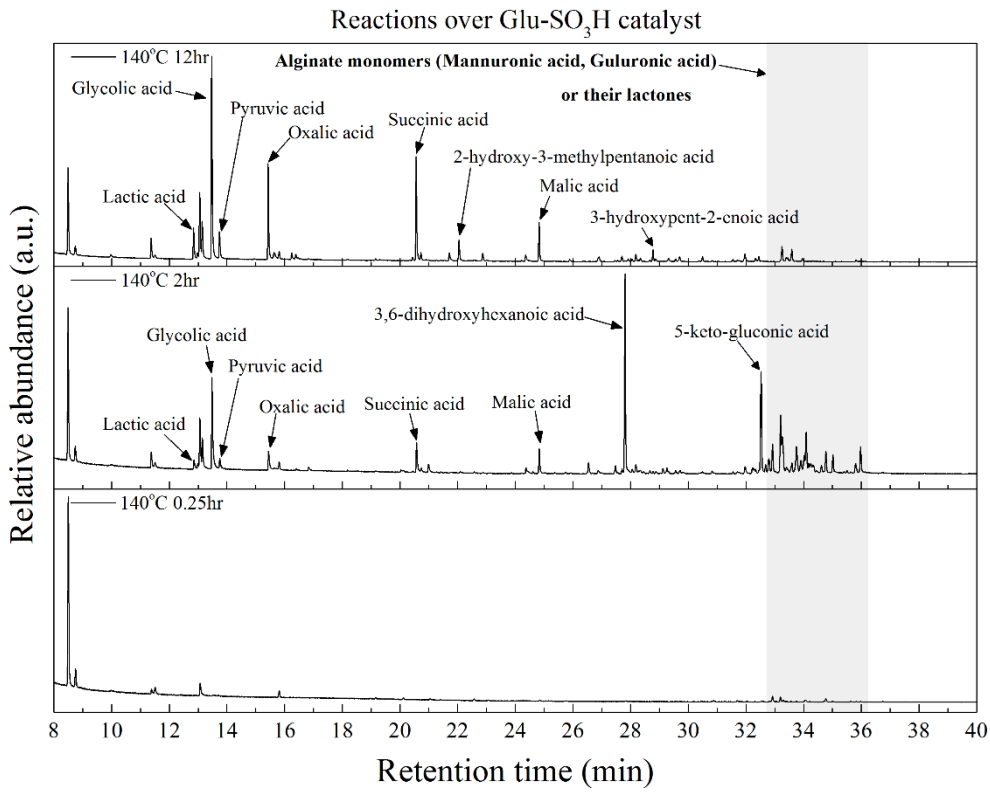

Figure 13. GC-MS total ion chromatograms of hydrolyzates reacted at 140℃ over Glu-SO_3H

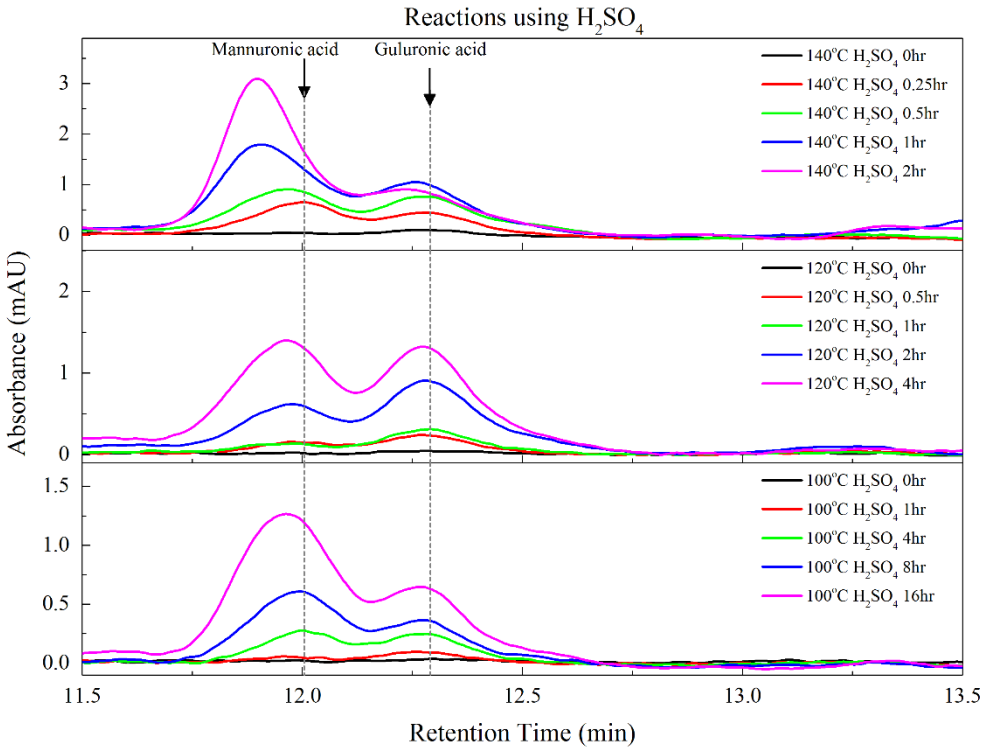

Figure 14. HPLC Chromatograms of reaction products hydrolyzed at different temperatures and times using H_2SO_4.

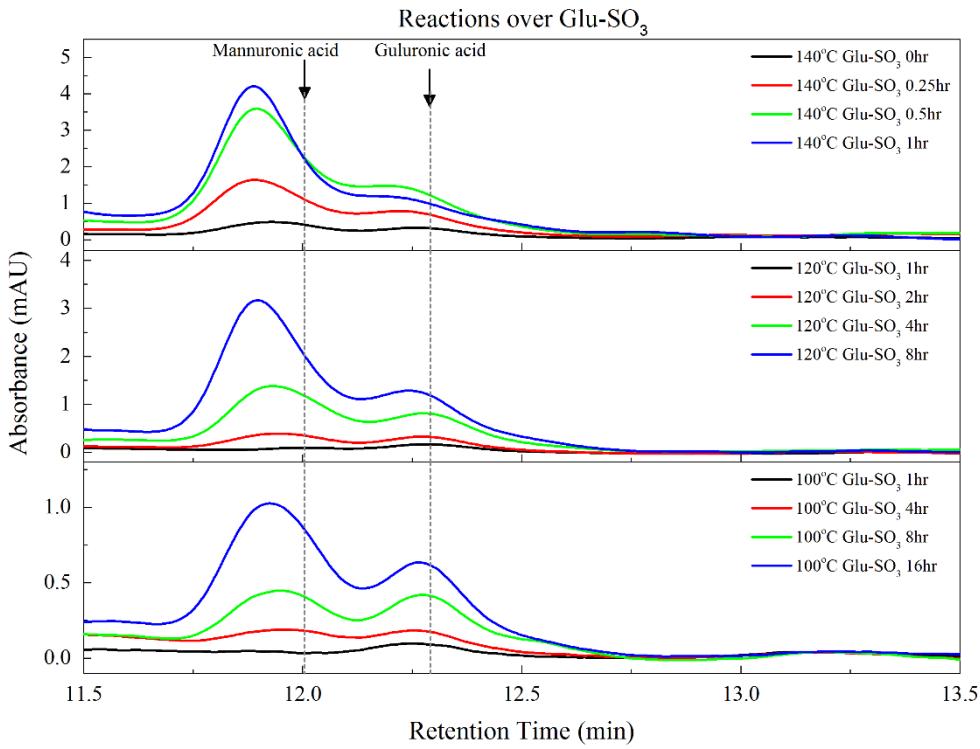

Figure 15. HPLC Chromatograms of reaction products hydrolyzed at different temperatures and times over Glu-SO_3

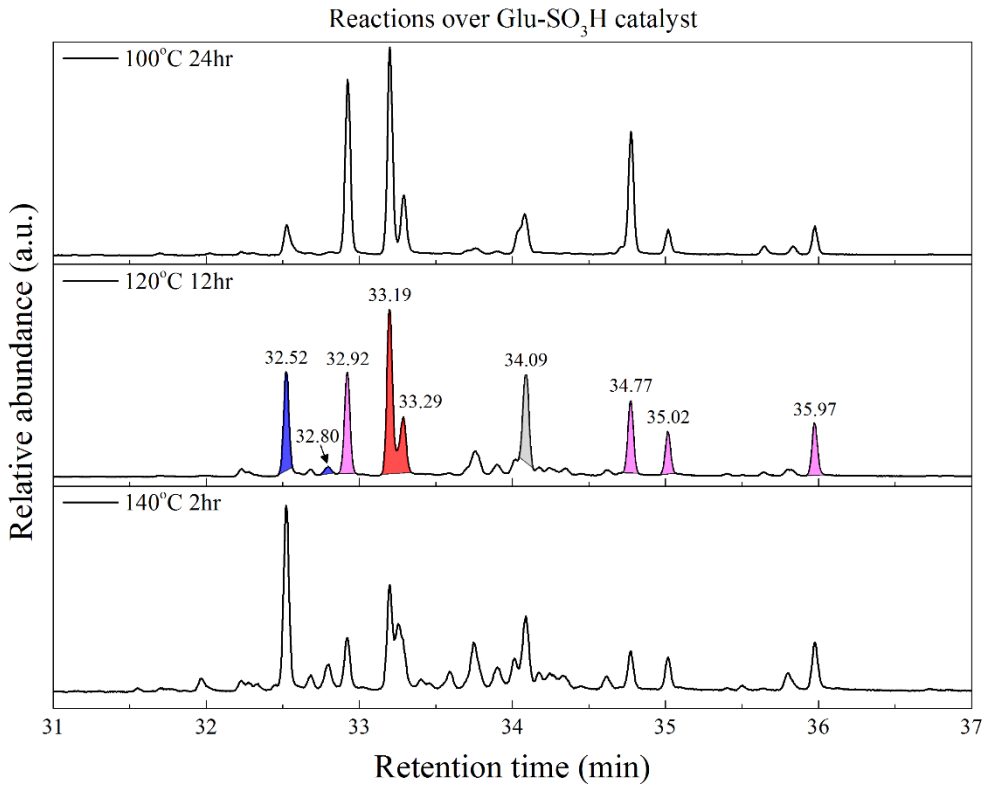

Figure 16. GC-MS total ion chromatograms of products reacted over Glu-SO_3H catalyst

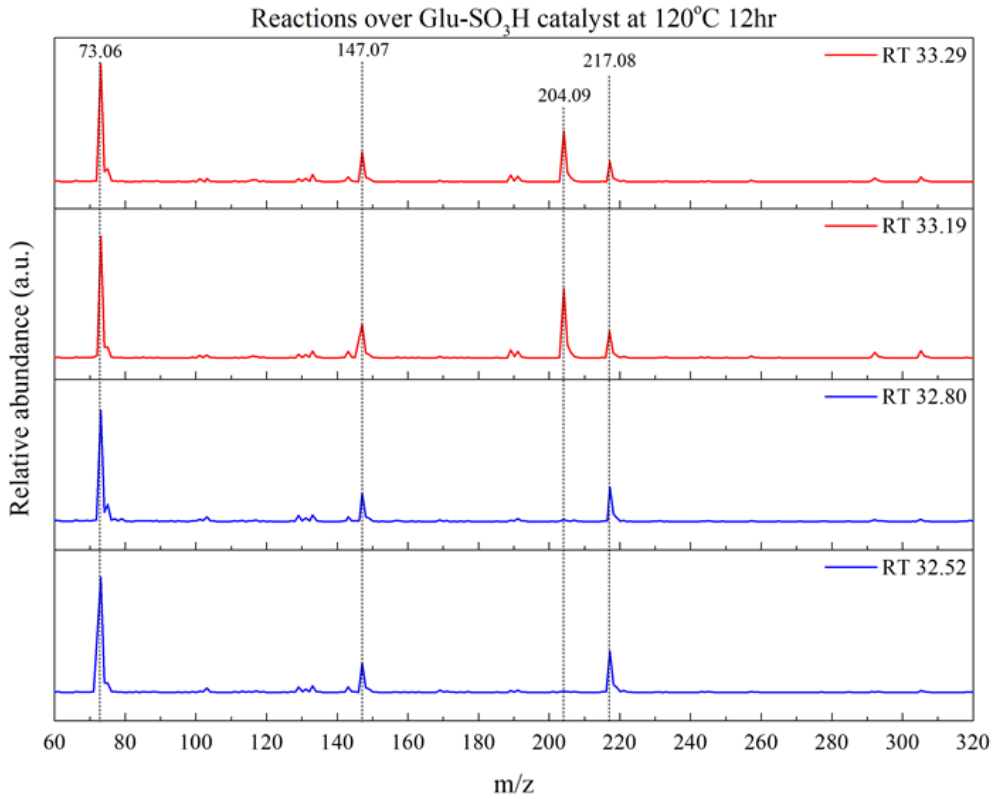

Figure 17. Mass spectra of GC-MS of the hydrolyzate reacted at 120℃ for 12hr

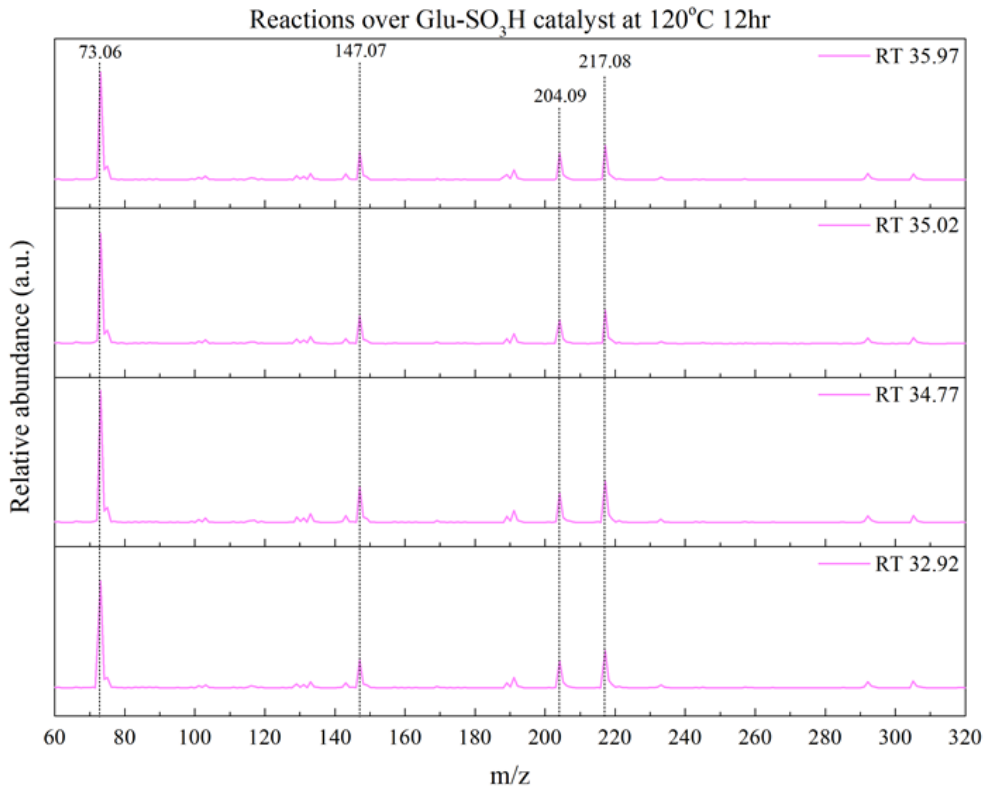

Figure 18. Mass spectra of GC-MS of the hydrolyzate reacted at 120℃ for 12hr

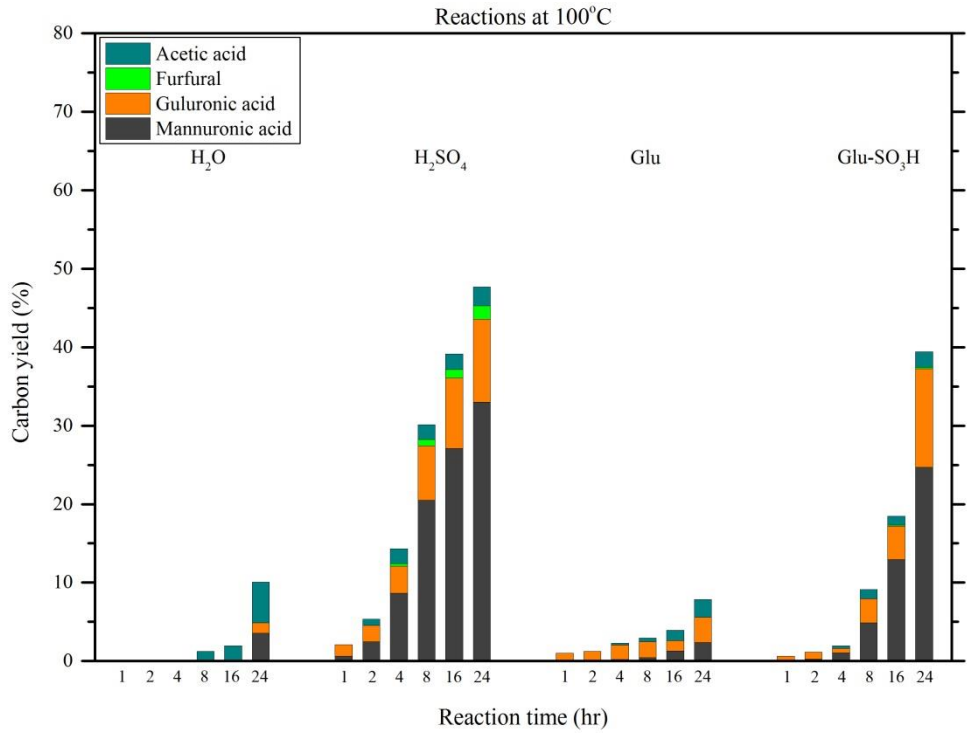

Figure 19. Product distribution for the hydrolysis of alginate using H_2SO_4 and the carbon catalysts at 100°C.

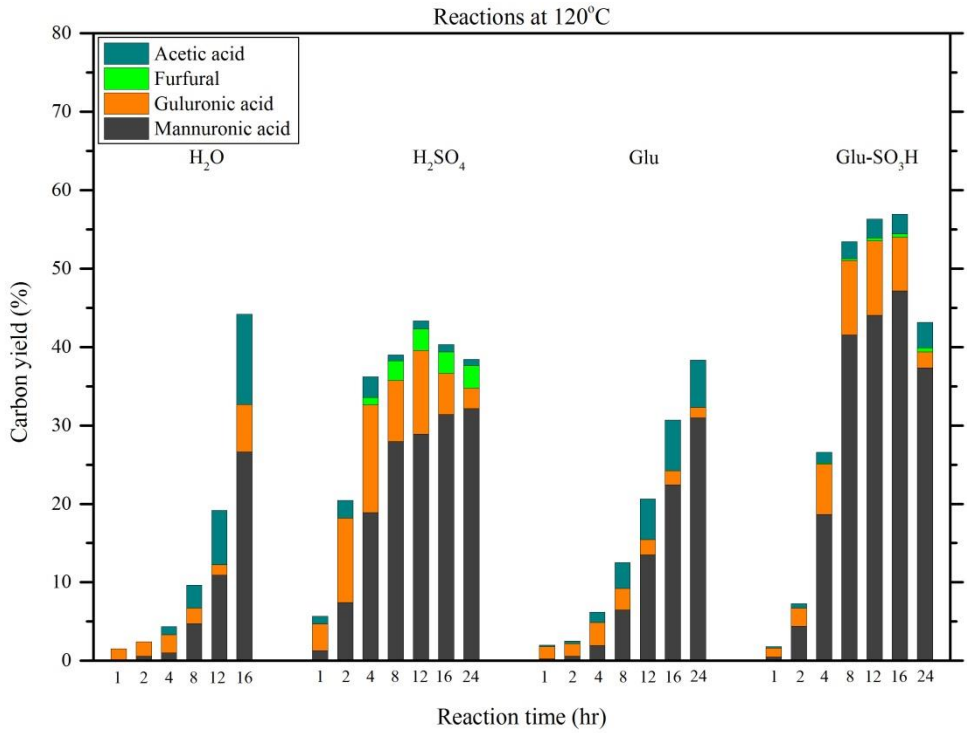

Figure 20. Product distribution for the hydrolysis of alginate using H_2SO_4 and the carbon catalysts at 120℃.

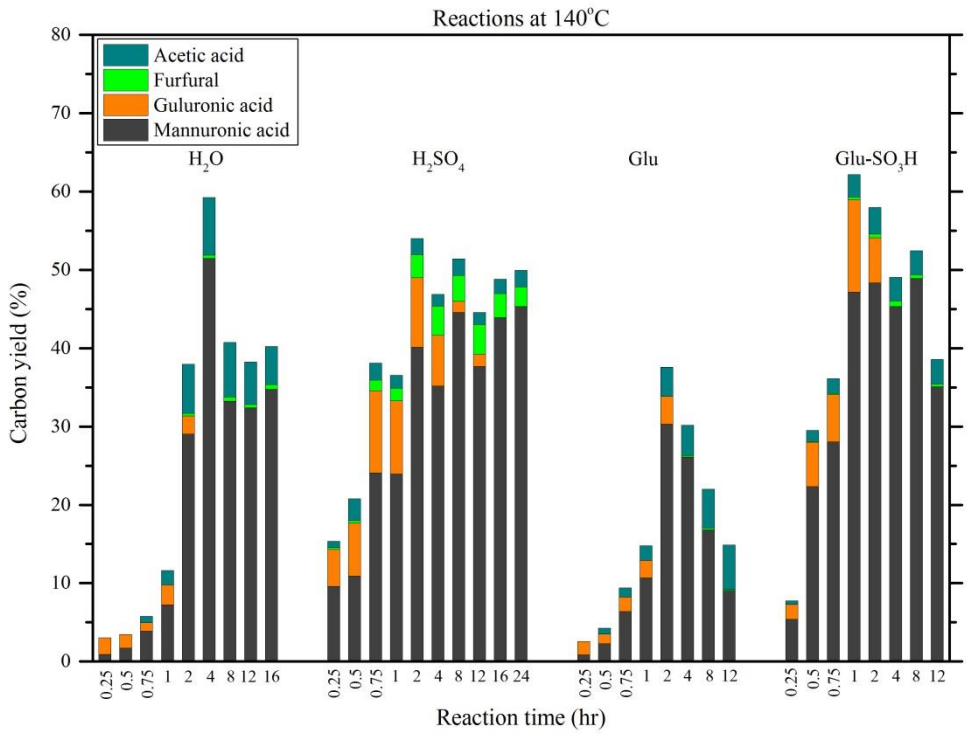

Figure 21. Product distribution for the hydrolysis of alginate using H_2SO_4 and the carbon catalysts at 140℃.

3.3. Hydrolysis of alginate over commercial solid acid catalysts

The hydrolysis was performed over different solid acid catalysts at 120 and 140℃ for 16 and 1hr, respectively. Acid density, surface area, and Si/Al ratio of commercial catalysts are summarized in Table 2. As shown in Figure 22 and 23, the Glu-SO_3H exhibits the highest total monomer yield with small amount of byproducts. Amberlyst15, a polymer comprised of polystyrene with $–SO_3H$, yielded high amount of byproducts, especially, furfural as in the case of sulfuric acid. Zeolite Y (CBV500 and CBV720) and MFI nanosponge zeolite show comparable catalytic activity with that of Glu-SO_3H at 120℃. The relatively high activity of zeolites is owing to large surface area. At 140℃, however, these zeolites lost their activity, which is attributable to collapse of zeolite structure under hydrothermal condition. Researches on hydrothermal stability of zeolites revealed that Al and Si species were dissolved into the high temperature liquid medium[66], and thus, most of them lost their structure[67] and showed poor hydrothermal stability.

From this comparison, the Glu-SO_3H catalyst is believed to be hydrothermally more robust than other solid acid catalysts examined. To further investigate the durability of the Glu-SO_3H catalyst, the catalyst reused up to four cycles at 140℃ for 1hr.

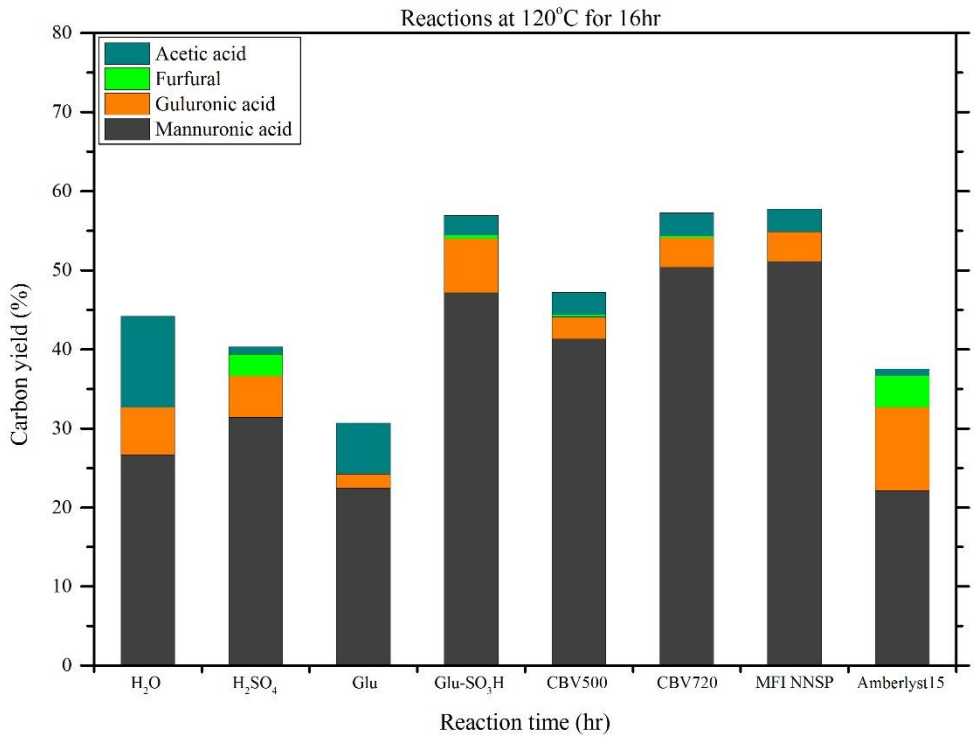

Figure 22. Product distribution for the hydrolysis of alginate over different catalysts at 120°C.

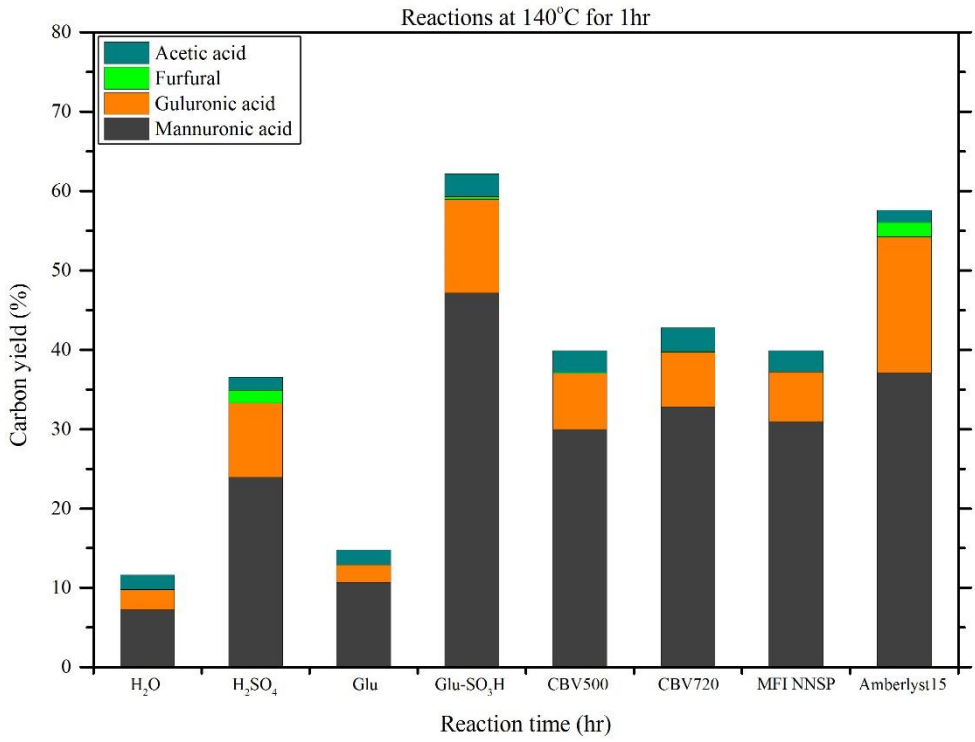

Figure 23. Product distribution for the hydrolysis of alginate over different catalysts at 140℃.

Table 2 Acid density, surface area of sulfuric acid, and Si/Al ratio of the carbon catalysts and other commercial solid acid catalyts

Catalyst	Acid density [a] (mmol/g)	Surface area (m^2/g)	Si/Al
Sulfuric acid	20.39	-	-
Glu	-	1.9	-
Glu-SO_3H	2.93	0.5	-
Amberlyst-15	2.99	45	-
MFI nanosponge	0.66	540	22
CBV500	0.15	750	5.2
CBV720	0.67	780	30

[a] Acid density was determined by back titration

3.4. Durability experiments of Glu-SO_3H catalyst

As shown in Figure 24, Glu-SO_3H catalyst lost its activity after repeated runs. However, the extent of activity loss decreases with each run. Although the catalytic activity was drastically dropped during the 1st and 2nd run, Glu-SO_3H maintained its activity since then. This was verified by ICP-AES (Table 3). The amount of sulfur leached decreases with each run. Compared to the fresh Glu-SO_3H, approximately 76% of sulfur was leached after the 4th run. The decrease in catalytic activities is in accordance with the loss of sulfur content from Glu-SO_3H. A method to prevent sulfur leaching is yet to be studied.

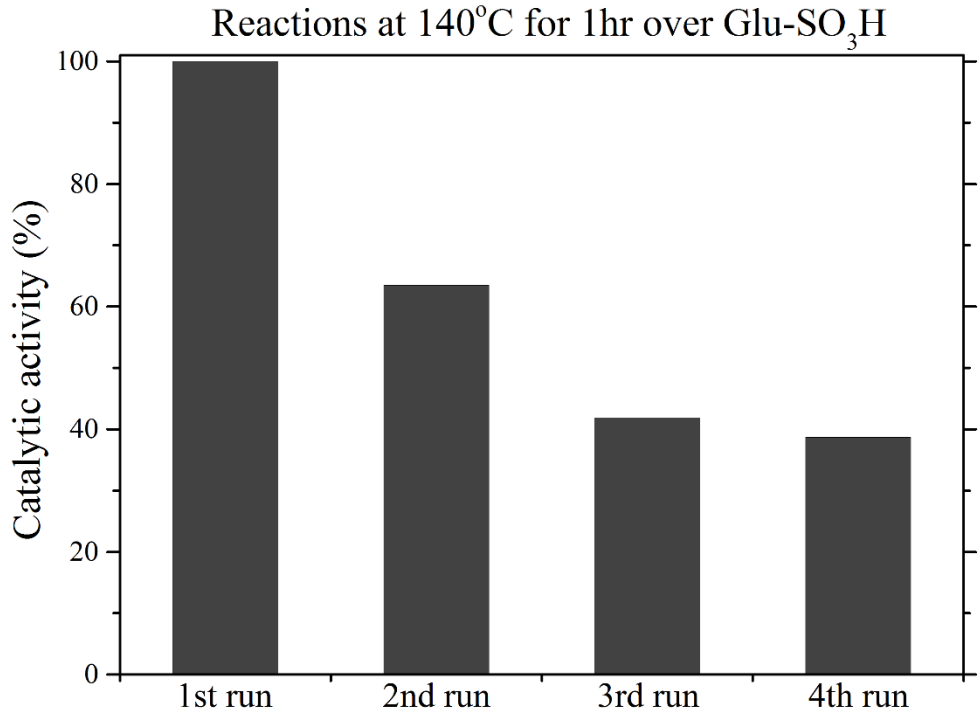

Figure 24. Catalytic activity of recycled Glu-SO_3H catalyst.

Table 3 Amount of Sulfur leached in aqueous products after the hydrolysis

Recycle run	Amount of S leached (mmol/g) [a]
0th run	0.767
1st run	0.301
2nd run	0.095
3rd run	0.093
4th run	0.097

[a] Sulfur contents in liquid products were determined by ICP-AES

Chapter 4. Conclusion

In this research, the sulfonated carbon catalyst was prepared by incomplete carbonization of glucose followed by sulfonation. The resultant carbon catalyst bearing –OH, –COOH, and $–SO_3H$ was employed to hydrolyze alginate into its monomers and compared to sulfuric acid and other commercial solid acid catalysts. The Glu-SO_3H catalyst showed a remarkable catalytic activity comparable with that of homogeneous acid catalyst, sulfuric acid, and the activity of prepared catalyst exceeded those of commercial solid acid catalysts yielding smaller amount of byproducts, acetic acid and furfural at all reaction temperatures. The superior activity is explained by high acid density and hydrophilic surface of the Glu-SO_3H catalyst, despite the relatively smaller surface area. Although sulfur was leached from the Glu-SO_3H during two cycles of hydrolysis, the catalyst maintained its activity since then.

References

1. Doman, L.E., *International Energy Outlook 2013.* U.S. Energy Information Administration, U.S. Department of Energy, 2013.
2. Birol, F., *World Energy Investment Outlook.* International Energy Agency, 2014.
3. *World Energy Outlook 2013.* International Energy Agency, 2013.
4. *The BP Energy Outlook 2035.* British Petroleum, United Kingdom, 2014.
5. Dincer, I., *Renewable energy and sustainable development: a crucial review.* Renewable and Sustainable Energy Reviews, 2000. **4**(2): p. 157-175.
6. Jacobson, M.Z. and M.A. Delucchi, *Providing all global energy with wind, water, and solar power, Part I: Technologies, energy resources, quantities and areas of infrastructure, and materials.* Energy Policy, 2011. **39**(3): p. 1154-1169.
7. Yu, Y., X. Lou, and H. Wu, *Some Recent Advances in Hydrolysis of Biomass in Hot-Compressed Water and Its Comparisons with Other Hydrolysis Methods†.* Energy & Fuels, 2007. **22**(1): p. 46-60.
8. Simmons, B.A., D. Loque, and H.W. Blanch, *Next-generation biomass feedstocks for biofuel production.* Genome biology, 2008. **9**(2): p. 242-242.
9. Lee, R.A. and J.-M. Lavoie, *From first- to third-generation biofuels: Challenges of producing a commodity from a biomass of increasing complexity.* Animal Frontiers, 2013. **3**(2): p. 6-11.

10. Chen, M., L. Xia, and P. Xue, *Enzymatic hydrolysis of corncob and ethanol production from cellulosic hydrolysate.* International Biodeterioration & Biodegradation, 2007. **59**(2): p. 85-89.

11. Bridgwater, A.V., *Review of fast pyrolysis of biomass and product upgrading.* Biomass and Bioenergy, 2012. **38**(0): p. 68-94.

12. Mohan, D., C.U. Pittman, and P.H. Steele, *Pyrolysis of Wood/Biomass for Bio-oil: A Critical Review.* Energy & Fuels, 2006. **20**(3): p. 848-889.

13. Shafizadeh, F., *Introduction to pyrolysis of biomass.* Journal of Analytical and Applied Pyrolysis, 1982. **3**(4): p. 283-305.

14. Meine, N., R. Rinaldi, and F. Schuth, *Solvent-free catalytic depolymerization of cellulose to water-soluble oligosaccharides.* ChemSusChem, 2012. **5**(8): p. 1449-54.

15. Harada, T., et al., *Hydrolysis of crystalline cellulose to glucose in an autoclave containing both gaseous and liquid water.* RSC Advances, 2014. **4**(51): p. 26838-26842.

16. Li, C. and Z.K. Zhao, *Efficient Acid-Catalyzed Hydrolysis of Cellulose in Ionic Liquid*. Advanced Synthesis & Catalysis, 2007. **349**(11-12): p. 1847-1850.

17. Rinaldi, R., R. Palkovits, and F. Schüth, *Depolymerization of Cellulose Using Solid Catalysts in Ionic Liquids.* Angewandte Chemie International Edition, 2008. **47**(42): p. 8047-8050.

18. Werpy, T.A., J.E. Holladay, and J.F. White, *Top Value Added Chemicals From Biomass: I. Results of Screening for Potential Candidates from*

Sugars and Synthesis Gas. U.S. Department of Energy, 2004.

19. Aida, T.M., et al., *Depolymerization of sodium alginate under hydrothermal conditions.* Carbohydrate Polymers, 2010. **80**(1): p. 296-302.
20. Matsushima, K., et al., *Decomposition reaction of alginic acid using subcritical and supercritical water.* Industrial & engineering chemistry research, 2005. **44**(25): p. 9626-9630.
21. Aida, T.M., et al., *Production of organic acids from alginate in high temperature water.* The Journal of Supercritical Fluids, 2012. **65**: p. 39-44.
22. Augst, A.D., H.J. Kong, and D.J. Mooney, *Alginate Hydrogels as Biomaterials.* Macromolecular Bioscience, 2006. **6**(8): p. 623-633.
23. Martinsen, A., G. Skjåk-Bræk, and O. Smidsrød, *Alginate as immobilization material: I. Correlation between chemical and physical properties of alginate gel beads.* Biotechnology and Bioengineering, 1989. **33**(1): p. 79-89.
24. Draget, K.I., G. Skjåk Bræk, and O. Smidsrød, *Alginic acid gels: the effect of alginate chemical composition and molecular weight.* Carbohydrate Polymers, 1994. **25**(1): p. 31-38.
25. Rowley, J.A., G. Madlambayan, and D.J. Mooney, *Alginate hydrogels as synthetic extracellular matrix materials.* Biomaterials, 1999. **20**(1): p. 45-53.
26. Murillo-Á lvarez, J.I. and G. Hernández-Carmona, *Monomer composition and sequence of sodium alginate extracted at pilot plant scale from three commercially important seaweeds from Mexico.* Journal of Applied

Phycology, 2007. **19**(5): p. 545-548.

27. Davis, T., et al., *1H-NMR study of Na alginates extracted from Sargassum spp. in relation to metal biosorption.* Applied Biochemistry and Biotechnology, 2003. **110**(2): p. 75-90.

28. Grasdalen, H., *High-field, 1H-n.m.r. spectroscopy of alginate: sequential structure and linkage conformations.* Carbohydrate Research, 1983. **118**(0): p. 255-260.

29. Grasdalen, H., B. Larsen, and O. Smidsrød, *A p.m.r. study of the composition and sequence of uronate residues in alginates.* Carbohydrate Research, 1979. **68**(1): p. 23-31.

30. Sartori, C., et al., *Determination of the cation content of alginate thin films by FTi.r. spectroscopy.* Polymer, 1997. **38**(1): p. 43-51.

31. Grant, G.T., et al., *Biological interactions between polysaccharides and divalent cations: The egg-box model.* FEBS Letters, 1973. **32**(1): p. 195-198.

32. Rousseau, I., et al., *Entrapment and release of sodium polystyrene sulfonate (SPS) from calcium alginate gel beads.* European Polymer Journal, 2004. **40**(12): p. 2709-2715.

33. Frush, H.L. and H. Isbell, *Preparation of mannuronic lactone from algin.* Journal of research of the National Bureau of Standards, 1946. **37**(5): p. 321-324.

34. Simensen, M.K., K. Draget, and F. Hjelland, *Procedure for producing uronic acid blocks from alginate*. 2000, Google Patents.

35. Sanchez-Machado, D.I., et al., *Determination of the uronic acid composition of seaweed dietary fibre by HPLC.* Biomed Chromatogr, 2004. **18**(2): p. 90-7.

36. Fu, Z., et al., *Preparation and catalytic performance of a carbon-based solid acid catalyst with high specific surface area.* Reaction Kinetics, Mechanisms and Catalysis, 2012. **107**(1): p. 203-213.

37. Fukuhara, K., et al., *Structure and Catalysis of Cellulose-Derived Amorphous Carbon Bearing SO3H Groups.* ChemSusChem, 2011. **4**(6): p. 778-784.

38. Guo, H., et al., *Cellulose-derived superparamagnetic carbonaceous solid acid catalyst for cellulose hydrolysis in an ionic liquid or aqueous reaction system.* Green Chemistry, 2013. **15**(8): p. 2167.

39. Hu, B., et al., *Functional carbonaceous materials from hydrothermal carbonization of biomass: an effective chemical process.* Dalton Transactions, 2008(40): p. 5414-5423.

40. Kitano, M., et al., *Preparation of a Sulfonated Porous Carbon Catalyst with High Specific Surface Area.* Catalysis Letters, 2009. **131**(1-2): p. 242-249.

41. Liu, M., et al., *Effective Hydrolysis of Cellulose into Glucose over Sulfonated Sugar-Derived Carbon in an Ionic Liquid.* Industrial & Engineering Chemistry Research, 2013. **52**(24): p. 8167-8173.

42. Mo, X., et al., *Activation and deactivation characteristics of sulfonated carbon catalysts.* Journal of Catalysis, 2008. **254**(2): p. 332-338.

43. Nakajima, K., M. Hara, and S. Hayashi, *Environmentally Benign Production of Chemicals and Energy Using a Carbon-Based Strong Solid Acid.* Journal of the American Ceramic Society, 2007. **90**(12): p. 3725-3734

44. Okamura, M., et al., *Acid-Catalyzed Reactions on Flexible Polycyclic Aromatic Carbon in Amorphous Carbon.* Chemistry of Materials, 2006. **18**(13): p. 3039-3045.

45. Onda, A., T. Ochi, and K. Yanagisawa, *Hydrolysis of Cellulose Selectively into Glucose Over Sulfonated Activated-Carbon Catalyst Under Hydrothermal Conditions.* Topics in Catalysis, 2009. **52**(6-7): p. 801-807.

46. Suganuma, S., et al., *Hydrolysis of cellulose by amorphous carbon bearing SO3H, COOH, and OH groups.* Journal of the American Chemical Society, 2008. **130**(38): p. 12787-12793.

47. Suganuma, S., et al., *Synthesis and acid catalysis of cellulose-derived carbon-based solid acid.* Solid State Sciences, 2010. **12**(6): p. 1029-1034.

48. Masakazu, T., T. Atsushi, and O. Mai, *Green chemistry: biodiesel made with sugar catalyst.* Nature, 2005. **438**: p. 178.

49. Hu, S., et al., *Efficient Hydrolysis of Cellulose over a Novel Sucralose-Derived Solid Acid with Cellulose-Binding and Catalytic Sites.* Journal of Agricultural and Food Chemistry, 2014. **62**(8): p. 1905-1911.

50. Guo, H., et al., *Hydrolysis of cellulose over functionalized glucose-derived carbon catalyst in ionic liquid.* Bioresource Technology, 2012. **116**(0): p. 355-359.

51. Shen, S., et al., *Preparation of a novel carbon-based solid acid from cocarbonized starch and polyvinyl chloride for cellulose hydrolysis.* Applied Catalysis A: General, 2014. **473**(0): p. 70-74.

52. Onda, A., T. Ochi, and K. Yanagisawa, *Selective hydrolysis of cellulose into glucose over solid acid catalysts.* Green Chemistry, 2008. **10**(10): p. 1033-1037.

53. Pang, J., et al., *Hydrolysis of cellulose into glucose over carbons sulfonated at elevated temperatures.* Chemical Communications, 2010. **46**(37): p. 6935-6937.

54. Zuo, Y., Y. Zhang, and Y. Fu, *Catalytic Conversion of Cellulose into Levulinic Acid by a Sulfonated Chloromethyl Polystyrene Solid Acid Catalyst.* ChemCatChem, 2014. **6**(3): p. 753-757.

55. Chambon, F., et al., *Cellulose hydrothermal conversion promoted by heterogeneous Brønsted and Lewis acids: Remarkable efficiency of solid Lewis acids to produce lactic acid.* Applied Catalysis B: Environmental, 2011. **105**(1-2): p. 171-181.

56. Tsubouchi, N., C. Xu, and Y. Ohtsuka, *Carbon Crystallization during High-Temperature Pyrolysis of Coals and the Enhancement by Calcium.* Energy & Fuels, 2003. **17**(5): p. 1119-1125.

57. Zong, M.-H., et al., *Preparation of a sugar catalyst and its use for highly efficient production of biodiesel.* Green Chemistry, 2007. **9**(5): p. 434-437.

58. Hara, M., et al., *A carbon material as a strong protonic acid.* Angew Chem Int Ed Engl, 2004. **43**(22): p. 2955-8.

59. Xie, X., et al., *Characterization of carbons derived from cellulose and lignin and their oxidative behavior.* Bioresource Technology, 2009. **100**(5): p. 1797-1802.

60. Jiang, Y., et al., *Acid functionalized, highly dispersed carbonaceous spheres: an effective solid acid for hydrolysis of polysaccharides.* Journal of Nanoparticle Research, 2011. **13**(2): p. 463-469.

61. Liu, X.-Y., et al., *Preparation of a Carbon-Based Solid Acid Catalyst by Sulfonating Activated Carbon in a Chemical Reduction Process.* Molecules, 2010. **15**(10): p. 7188-7196.

62. Pang, Q., et al., *Cellulose-derived carbon bearing -Cl and -SO3H groups as a highly selective catalyst for the hydrolysis of cellulose to glucose.* RSC Advances, 2014. **4**(78): p. 41212-41218.

63. Shuai, L. and X. Pan, *Hydrolysis of cellulose by cellulase-mimetic solid catalyst.* Energy & Environmental Science, 2012. **5**(5): p. 6889.

64. Mao, S., et al., *The depolymerization of sodium alginate by oxidative degradation.* Pharmaceutical development and technology, 2012. **17**(6): p. 763-769.

65. Akiya, N. and P.E. Savage, *Roles of water for chemical reactions in high-temperature water.* Chemical Reviews, 2002. **102**(8): p. 2725-2750.

66. Kruger, J.S., V. Nikolakis, and D.G. Vlachos, *Aqueous-phase fructose dehydration using Brønsted acid zeolites: Catalytic activity of dissolved aluminosilicate species.* Applied Catalysis A: General, 2014. **469**(0): p. 116-123.

67. Zapata, P.A., et al., *Hydrophobic Zeolites for Biofuel Upgrading Reactions at the Liquid–Liquid Interface in Water/Oil Emulsions.* Journal of the American Chemical Society, 2012. **134**(20): p. 8570-8578.

요약 (국문초록)

환경오염을 완화시키고 석유기반 연료 및 화학 물질에 대한 의존도를 낮추기 위하여, 농작물, 목본계, 해조류 등의 다양한 바이오매스 자원이 연구되었다. 이러한 바이오매스 원료 중 빠른 성장 속도를 가진 해조류는 식량 문제와 상충되지 않고, 분해가 어려운 리그닌 성분이 없기 때문에 차세대 바이오매스 자원으로 각광받고 있다.

해조류의 주성분인 알지네이트는 다양한 산업에서 사용되고 있다. 글루코오즈의 1,4-glycosidic 결합으로 이루어진 셀룰로오즈처럼, 알지네이트는 β-D-글루론산과 α-D-만루론산의 두 단량체가 1,4-glycosidic 결합으로 이루어져있다. 이러한 구조적 유사성 때문에 알지네이트는 고부가가치 화학물질을 생산하기 위해 수열분해와 같은 기존의 바이오리파이너리 공정에 직접 이용될 수 있다. 바이오매스 자원을 효과적으로 가수분해시키기 위해서는 산 촉매의 사용이 필수적이다. 그러나 황산 혹은 염산과 같은 균일계 촉매의 사용은 촉매와 생성물의 분리, 생성물 정제, 폐기물 중화 등의 문제를 야기시킨다. 따라서, 쉽게 분리가 가능하고 높은 촉매적 활성을 갖는 고체 산 촉매를 개발하는 것이 세계적 관심사로 대두되었다.

본 연구에서는 알지네이트를 수열분해하여 단량체를 생산하기 위하여 술폰기가 도입된 글루코오즈 유래 카본 촉매를 사용하였다. 합성된

카본 촉매의 산 농도, 표면적, 열적 안정성 등이 단량체 수율에 미치는 영향을 알아보았다. 글루코오즈의 불완전 탄화 및 술폰화를 통해 합성된 촉매는 phenolic OH, –COOH, $-SO_3H$의 세 가지 작용기를 지니게 된다. 강한 브뢴스테드 산점($-SO_3H$)이 알지네이트의 가수분해반응을 촉진시키지만 약한 산점(–OH와 –COOH)은 알지네이트 분해에 미미한 영향을 미치는 것으로 확인되었다. 작은 표면적을 가지고 있음에도 불구하고, 술폰산이 기능화된 카본 촉매가 황산과 견줄만한 높은 활성을 갖는 이유는 촉매의 친수성 표면과 높은 산 농도에 기인한다. 술폰기가 도입된 글루코오즈 유래 카본 촉매는 균일계 촉매를 대체할 차세대 고체 산 촉매로서 알지네이트, 더 나아가 바이오매스 원료를 효과적으로 분해할 수 있는 가능성을 보여주었다.

주요어 : 알지네이트 가수분해, 만루론산, 글루론산, 술폰기가 도입된 카본 촉매

학 번 : 2013-20973